CHEMICAL PHYSICS 6 (1974) 205–216. © NORTH-HOLLAND PUBLISHING COMPANY

IONIZATION AND FRAGMENTATION OF ANILINE AND OTHER ORGANIC MOLECULES IN COLLISION WITH HALOGEN ATOMS IN THE ELECTRONVOLT ENERGY RANGE

G.P. KÖNNEN, J. GROSSER *, A. HARING, F. EERKENS,
A.E. DE VRIES and J. KISTEMAKER
FOM-Instituut voor Atoom- en Molecuulfysica, Amsterdam/Wgm., The Netherlands

Received 30 July 1974

Ionization and fragmentation of aniline, n-propylbenzene, carbontetrachloride, benzene, propane and cylcohexane is studied under halogen impact. The energy dependences of the ionization cross sections of aniline in collisions with halogens are reported. The results show an analogy with electron impact and photo-ionization mass spectroscopy. They are discussed in terms of potential curve crossings in the halogen–organic molecule system.

1. Introduction

Since the electronvolt region has been opened for neutral atom beams, a number of papers has been published on the different aspects of collisional ionization. The research has been mainly restricted to alkali collisions with monatomic or diatomic particles [1]. In order to study fundamental chemical processes of organic molecules, we extended the sputtering technique to alkali-halide targets and thereby obtained hyperthermal halogen beams [2]. In the present paper we report measurements on the ionization and fragmentation of aniline ($C_6H_5NH_2$) and some other organic molecules in collision with these hyperthermal halogen beams.

2. Experimental method

The apparatus used for the present experiments has been described previously in detail [2,3]. A schematic view of the relevant parts of this apparatus is given in fig. 1. Neutral particles are sputtered from alkali-halide surfaces by a chopped 6 keV Ar^+ ion beam. After mechanical velocity selection and collimation they are crossed with a thermal beam. Ions formed in the collision center are extracted by a homogeneous electric field, pass a mass spectrometer and are counted on a particle multiplier with a forward–backward counter.

Data on the composition of beams sputtered from alkali-halide surfaces and on the energy dependence of the beam intensity have been reported earlier [2]. At the velocities which are required for the present experiments, the beam consists only of alkali and halogen atoms and a small amount of alkali-halide molecules. Evidence that the observed ions are only produced with the halogen constituent of the sputtered beam is taken from the fact that we find identical results with beams sputtered from NaCl, KCl or CsCl targets: Threshold velocities for collisional ionization with aniline ($C_6H_5NH_2$) are found to be the same within the experimental uncertainty for all these cases. Furthermore, the ion yields as a function of the velocity of the sputtered beam are identical for NaCl, KCl and CsCl. This is in agreement with our earlier statement [2] that the energy distributions of for instance Cl atoms sputtered from different alkali-halide surfaces are identical at eV energies. Another check consisted of producing a hyperthermal beam of potassium atoms by sputtering from a potassium target and crossing it with an aniline beam. Neither positive aniline ions

* Present address: Institut C für Experimentalphysik, Technische Universität, Appelstrasse 1, Hannover, Germany.

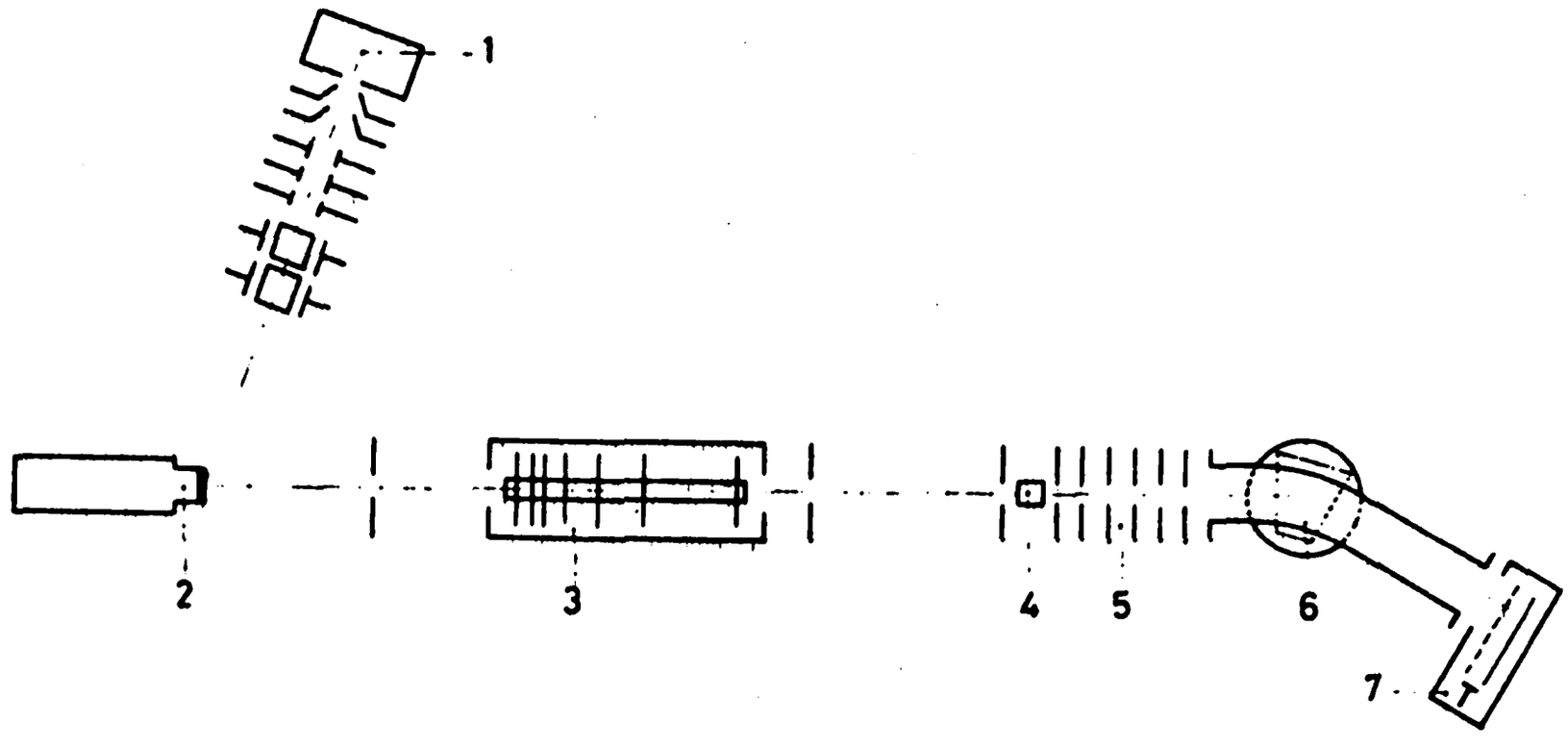

Fig. 1. Schematic view of the apparatus. (1) Ion source, (2) targetholder, (3) mechanical velocity selector, (4) collision region, (5) extraction field, (6) magnet, (7) multiplier.

nor positively charged fragments were observed in this case.

The thermal beam effuses from a multichannel array (channel diameter 12 μ, channel length 480 μ, surface 0.18 cm^2) and is shot directly into a liquid nitrogen trap. Typical working conditions in the mass spectrometer are: pressure before multichannel array 0.1 torr, background pressure caused by the thermal beam 5×10^{-5} torr, extraction voltage of the ions 1100 V. At working condition, the thermal beam has a small angular spread and the collision region is well defined.

The velocity selector has been calibrated by measuring the threshold of the process $K + Br_2 \rightarrow K^+ + Br^- + Br - 2.95$ eV [4]. We estimated the error in the velocity calibration to be 0.3%. The resolution of the velocity sector $\Delta v/v$ is about 10%.

There are two instrumental effects which can cause errors in our results. Firstly, because of the poor resolution of the mass spectrometer ($m/\Delta m \approx 20$) the determination of the observed mass numbers is only correct within $\Delta m = \pm 1$. The exact values of the mass numbers of the measured ions were taken from the analogy with ordinary mass spectroscopy (see section 3.1). Although this procedure will be correct at low energies, where only a small number of fragment ions can be formed, it cannot be excluded that at higher energies a given mass spectrometer peak includes various neighbouring masses. No errors arise in connection with initial kinetic energy of the ions, and all ions of a given mass formed in the collision are indeed measured on the collector, as has been checked experimentally. Secondly, since there are also ionizing collisions in the acceleration field in the mass spectrometer, all peaks have a low intensity tail in the direction of lower mass numbers. It is probably due to this disturbing effect that some of the ions give a low positive signal below threshold. In most cases, it is negligible however. Small positive signals below threshold may also originate from collisions of sputtered alkali-halide molecules with the thermal beam.

3. Results

3.1. Non-velocity selected spectra

Non-velocity selected beams of halogens X have been crossed with various thermal beams of organic molecules Y and the mass spectra of the formed positive ions have been recorded. The observed mass numbers are given in table 1. The alkali-halide targets MX from which the halogen beams were sputtered also have been indicated in table 1. Fragment ions with mass near M could not be observed because they are obscured by the process $MX + Y \rightarrow M^+ + X^- + Y$ [2].

The mass numbers in table 1 agree closely with the main singly charged fragments observed in electron mass spectroscopy [5]. No differences have been found in the mass numbers of the products arising from collisions with different halogens. This indicates that the processes occurring in halogen collisions are closely related to electron impact ionization and fragmentation. A similar relation seems to exist for negative

Table 1
Mass numbers of positive ions arising from collisions of halogen atoms with organic molecules. The targets which are used to generate the hyperthermal halogen beams are indicated in parentheses. For aniline, only the halogen is indicated since for each halogen several experiments have been done with various alkali halide targets.

(F, Cl, Br, I) aniline	93	66	52	39	28		
(NaCl) propane	42	28	15				
(NaCl) cyclohexane	85	56	41	28			
(KF, NaCl) carbontetrachloride	118	80	47				
(NaCl) benzene	79	64	52	39			
(NaCl) n-propyl benzene	121	91	78	66	51	39	28

ion formation, since alkali–SF_6 collisions give rise to the same charged products as negative mass spectroscopy [6].

The relative intensities of the fragments are not given in table 1. Actually, these quantities cannot be compared entirely with the data of electron impact, since the measured ion yield of non-velocity selected beams is given by the convolution of the cross section with the energy distribution of the sputtered beam, which varies roughly with E^{-2} at electronvolt energies [2]. Nevertheless, the observed relative intensities show the same tendency as in electron impact.

3.2. Velocity selected spectra

The energy dependence of the ionization cross section of various positively charged fragments of the system F, Cl, Br and I with aniline ($C_6H_5NH_2$) are given in figs. 2–5.

The solid line in fig. 3 represents the gross ionization cross section, which is the sum over all fragments. For Br and I not all fragments could be measured because the signals were too low. The abscissa of the figures represent the center of mass energies of the halogen–aniline systems, calculated from the velocity of the sputtered beam and averaged over the naturally occurring isotopes. The energy dependence of the cross sections is obtained by dividing the counting rates by the flux of the sputtered beam. Flux distributions of Cl, Br and I have been measured directly [2]. For F sputtered from KF, the flux distribution was taken to be identical [2] to that of Na sputtered from NaCl. This latter distribution was measured by surface ionization detection. The experimental uncertainty in the flux distribution of the primary beams can cause an error of less than 20% in the cross sections at the higher energies in figs. 2–5.

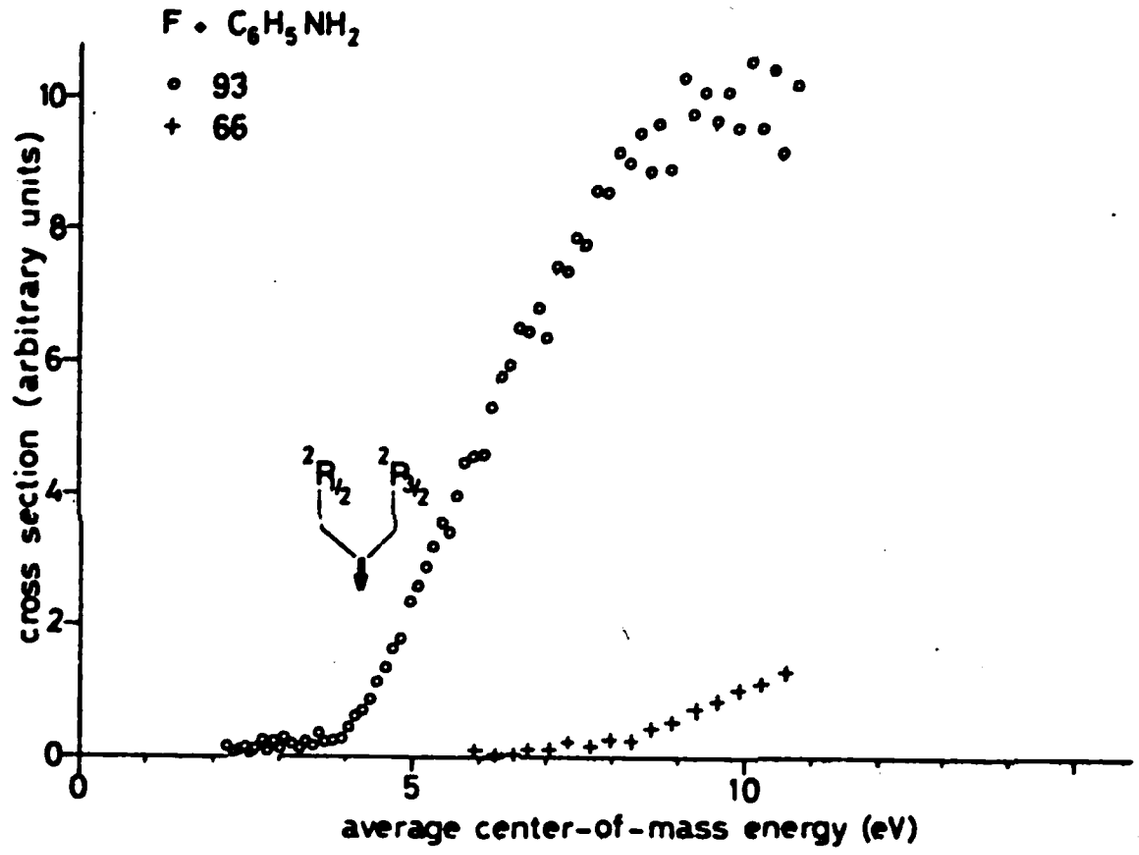

Fig. 2. Cross sections for production of positive ions if F atoms collide on aniline. The centre of mass energy is averaged over the different isotope combinations. The mass 93 ion is the parent ion.

The height of the observed signals of the parent peak (mass 93) decreases from F to I; the signals for F are about a factor of twenty higher than for I. From the flow of the sputtered beams we estimate the cross section to be in proportion to roughly 2:1:0.5:0.3 for F:Cl:Br:I. Comparing the aniline signals with the signals obtained from the process $K + Br_2 \rightarrow K^+ + Br_2^-$ we estimate the ionization cross sections for Cl on aniline to be about 2% of the latter process at 7000 m/s. This corresponds with an absolute value in the order of 0.1–1 $Å^2$ [7].

The chemical composition of the fragments cannot be deduced from our experiments. From electron impact mass spectroscopy [8,9] one concludes that the products are mainly non-nitrogen containing compounds, originating from HCN loss. Although the mass 66 fragment in photoionization is reported to be

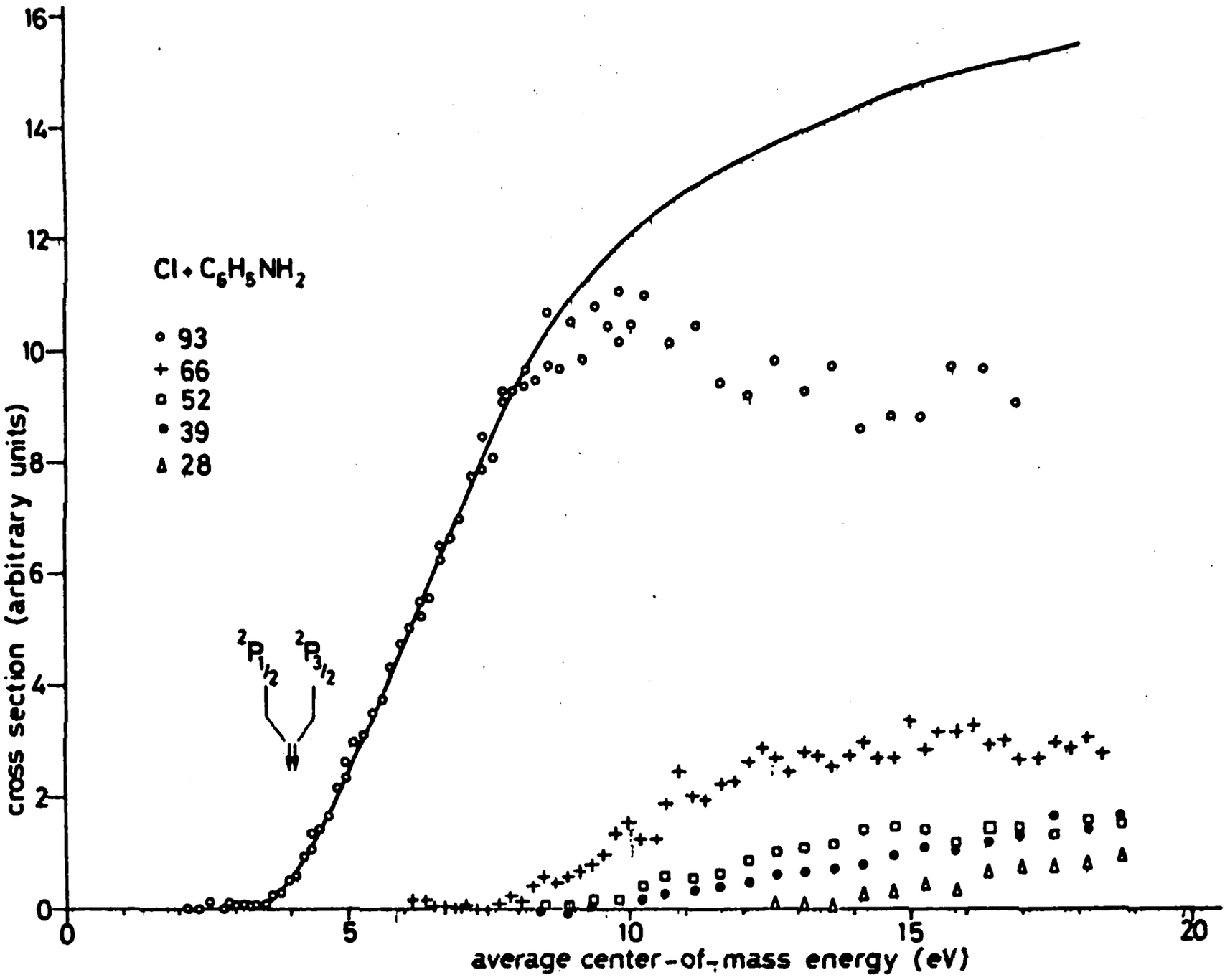

Fig. 3. Cross sections for production of positive ions if Cl atoms collide on aniline. The centre of mass energy is averaged over the different isotope combinations. The gross ionization cross section (summed over all fragments) is indicated by a solid line. The mass 93 ion is the parent ion.

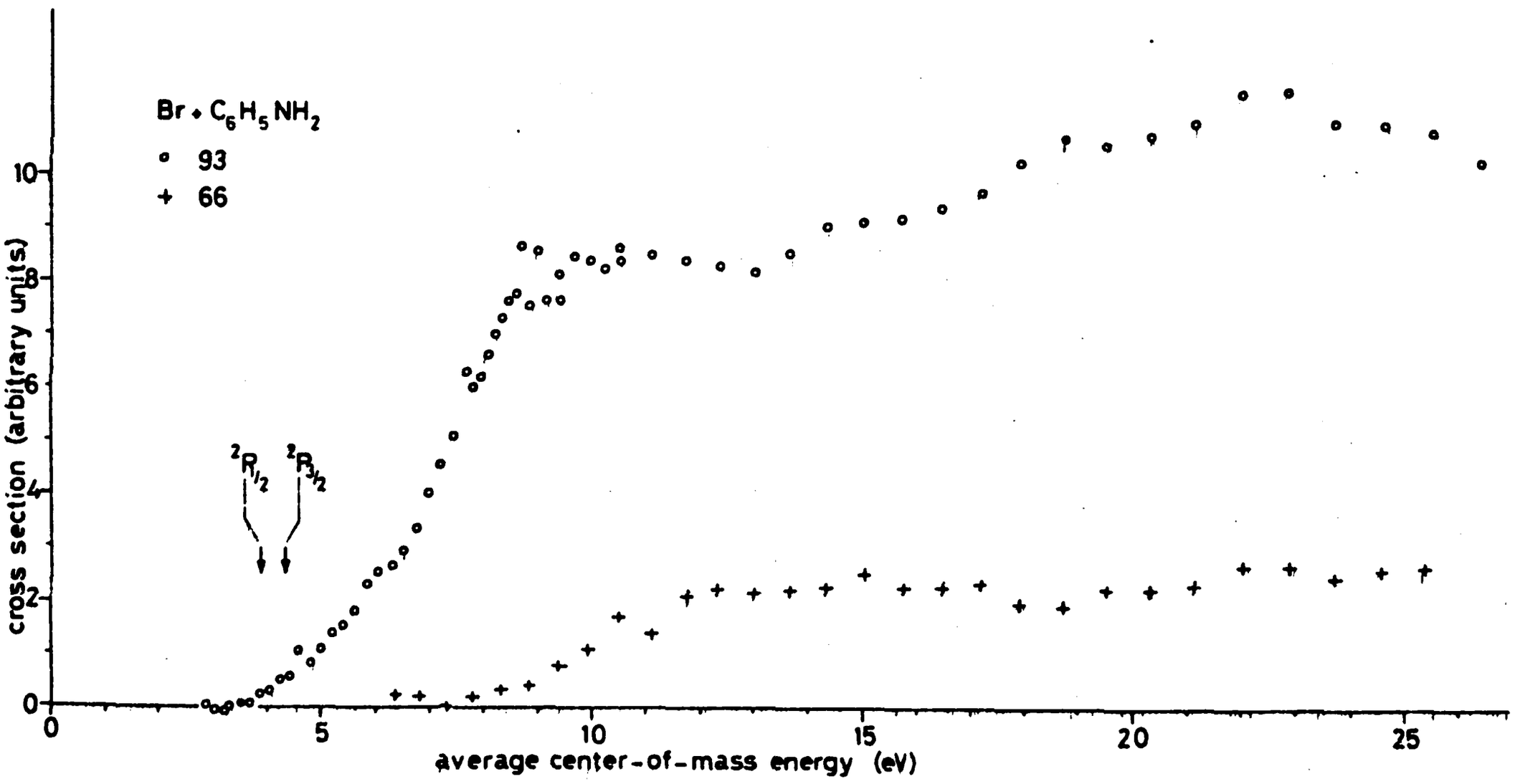

Fig. 4. Cross section for production of positive aniline ions and the fragment ion with mass 66 if Br atoms collide on aniline. The centre of mass energy is averaged over the different isotope combinations.

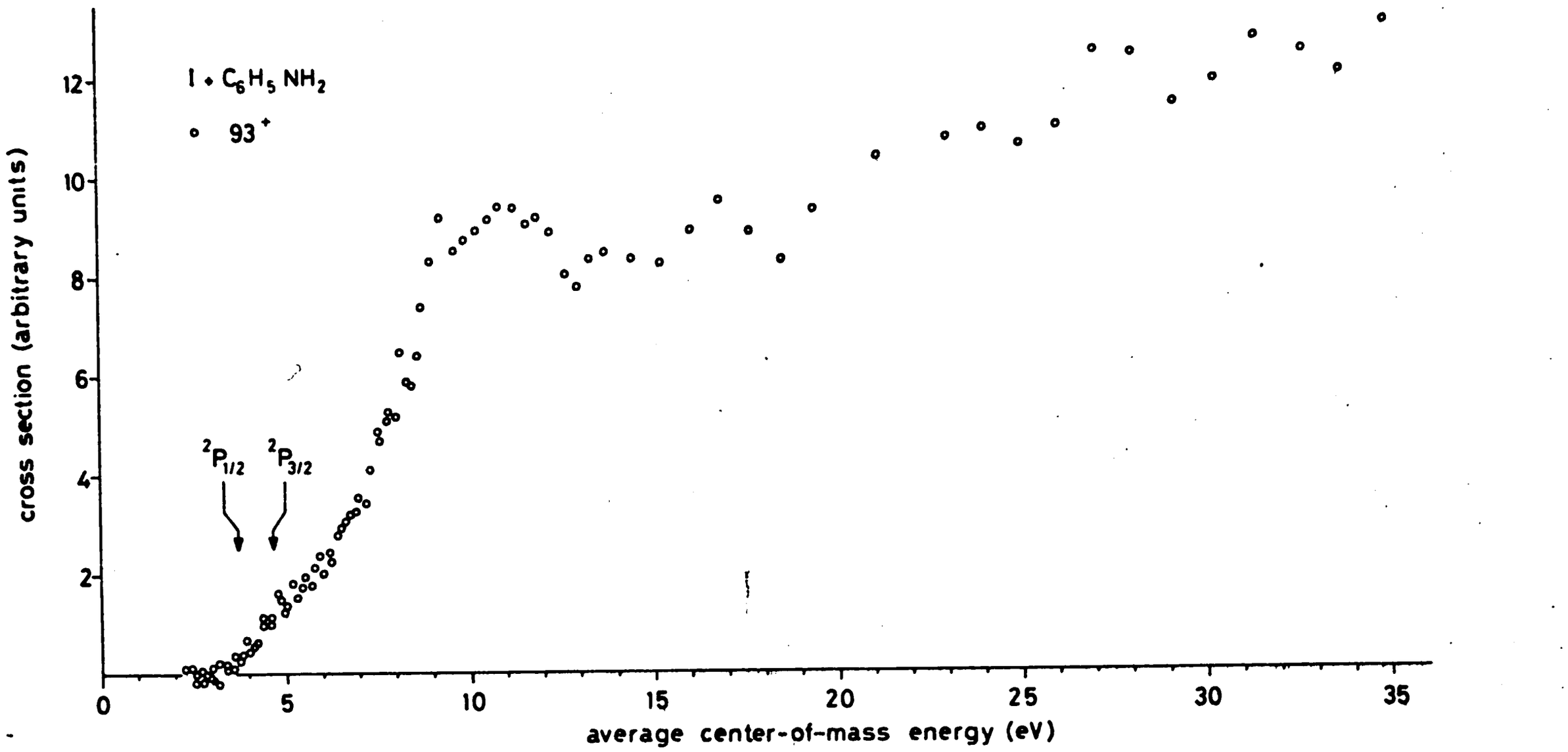

Fig. 5. Cross section for production of positive aniline ions if I atoms collide on aniline. The centre of mass energy is averaged over the different isotope combinations.

an exception [10] a recent electron impact experiment [11] showed that also for low energies this fragment is a hydrocarbon. Adopting this result, the formula of the fragments with mass 28, 39, 52 and 66 are $C_2H_4^+$, $C_3H_3^+$, $C_4H_4^+$ and $C_5H_6^+$, respectively.

Estimating roughly the thresholds for the parent peak in figs. 2–5 we found them to be in good agreement with the values expected from the ionization potential of aniline [10] and the electron affinity of the halogens [12] in the cases of Cl and F. For Br and I however, the experimental thresholds were too low by about 0.4 and 1 eV respectively. We ascribe this effect to the presence of long living $^2P_{1/2}$ excited halogens in the sputtered beam. The ground states are $^2P_{3/2}$. This explains both the agreement of the Cl and F results and the deviation of the Br and I threshold. The $^2P_{1/2}$ state lies 0.05, 0.11, 0.46 and 0.94 eV above the ground state of F, Cl, Br and I respectively [13]. From the fact that no signal is observed below the $^2P_{1/2}$ threshold we conclude that the $^2P_{1/2}$ atoms are the only excited halogen atoms in the beams.

3.3. Threshold energies

In this section first the various experimental effects that influence the threshold behaviour are discussed. Then we describe how the threshold energies are inferred from the experimental results; the values are reported in table 2.

It is assumed that the ideal ionization cross section for a certain halogen atom and aniline molecule as a function of the velocity is a straight line beginning at threshold. We define the threshold velocity of a process as the *principal threshold* if the following conditions are satisfied:

(1) the thermal beam has zero velocity;

(2) both colliding particles are in their ground state;

(3) both particles have their most abundant mass number, so H = 1, C = 12, N = 14, F = 19, Cl = 35 and I = 127. We take however 80 in case of Br.

The *experimental threshold*, found by extrapolating the straight part of the cross section curve, will be shifted with respect to the principal threshold because of the following reasons:

1. Vibrational excitation of the molecules in the thermal beam. The thermal distribution of the vibra-

tional states has to be known. For the aniline molecule, these were estimated from the known states of benzene [14].

2. Halogen projectiles in the metastable $^2P_{1/2}$ state. Since information is lacking, we assume that 50% of the halogen atoms are in the $^2P_{1/2}$ state. This will lead to an uncertainty of less than 0.1 eV for the Br results. For I, the principal threshold was calculated from the $^2P_{1/2}$ threshold.

3. The velocity of the thermal beam. Its magnitude is known at room temperature, its angular spread can be neglected.

4. Isotope shift. The threshold velocity is different for different isotope combinations. The distribution of isotopes is well known for both colliding particles.

All these effects change the threshold velocity by at most a few percent, except in case of the Br and I metastables, as mentioned before. All combinations of masses and excited states (point 1, 2 and 4) have threshold velocities different from the principal threshold. For a delta-shaped velocity distribution the experimental ionization cross section $\sigma_1(v)$ will therefore be a superposition of several pieces of straight lines. If the slope of the cross section is supposed to be the same for all processes, the slope of $\sigma_1(v)$ is enlarged by an amount proportional to the probability of the new process at every new threshold. This probability of course equals the relative abundance of the colliding particles for which the threshold is reached. Above the highest threshold, $\sigma_1(v)$ will be a straight line again. The extrapolation of this line will in general not intersect the x-axis at the principal threshold velocity.

To deduce the expected experimental cross section from $\sigma_1(v)$, this function has to be convoluted with the resolution function of the velocity selector, $R(v, v_0)$, v_0 being the nominal velocity of the selector. The resulting function will be called $\sigma_2(v_0)$. Thus

$$\sigma_2(v_0) = \int R(v, v_0)\, \sigma_1(v)\, dv . \qquad (1)$$

This function is also a straight line above the threshold region. The intersection of its extrapolation is the same as for $\sigma_1(v)$ in our case, as can be shown as follows.

For mechanical velocity selectors, $R(v, v_0)$ depends only on v/v_0 [15]. Let $R(v, v_0)$ be non-zero if $1-a < v/v_0 < 1+b$, a and b being constants. Because of normalization one has

$$\int_{v_0(1-a)}^{v_0(1+b)} R(v, v_0)\, dv = 1 . \qquad (2)$$

On the right hand side of the threshold region, $\sigma_1(v)$ is a straight line. Let v_D be the intersection with the x-axis of its extrapolation. Then in this region we have $\sigma_1(v) \propto v - v_D$. Consequently one gets from (1)

$$\sigma_2(v_0) \propto \int_{v_0(1-a)}^{v_0(1+b)} (v - v_D)\, R(v, v_0)\, dv$$

$$= \int_{v_0(1-a)}^{v_0(1+b)} (v - v_0 + v_0 - v_D)\, R(v, v_0)\, dv$$

$$= (v_0 - v_D) \int_{v_0(1-a)}^{v_0(1+b)} R(v, v_0)\, dv$$

$$+ \int_{v_0(1-a)}^{v_0(1+b)} (v - v_0)\, R(v, v_0)\, dv$$

$$= v_0 - v_D + \int_{v_0(1-a)}^{v_0(1+b)} (v - v_0)\, R(v, v_0)\, dv . \qquad (3)$$

Substituting in the remaining integral $w = v - v_0$, one finds

$$\sigma_2(v_0) \propto v_0 - v_D + \int_{-av_0}^{bv_0} w\, R(v_0 + w, v_0)\, dw . \qquad (4)$$

The resolution function $R(v, v_0)$ of the mechanical velocity selector is within a good approximation a symmetrical triangle around v_0 [15]. This implies that $a = b$. Since in this case the integrand in (4) is anti-symmetric, the resulting integral is zero. So the intersection of the extrapolated straight part will be indeed v_D. The reported slight asymmetry in $R(v, v_0)$ ($a = 0.10$, $b = 0.11$) will give rise to a negligible shift of the intersection of $\sigma_2(v_0)$ of about 0.3% of v_D to a higher velocity. This error however is entirely compensated by the fact that the calibration of the selector is also done with a known linear cross section. For the actual calculation of the threshold energy, the function $\sigma_1(v)$ was constructed, starting with a reasonably guessed principal threshold. The ratio of the principle threshold and the value at which the extra-

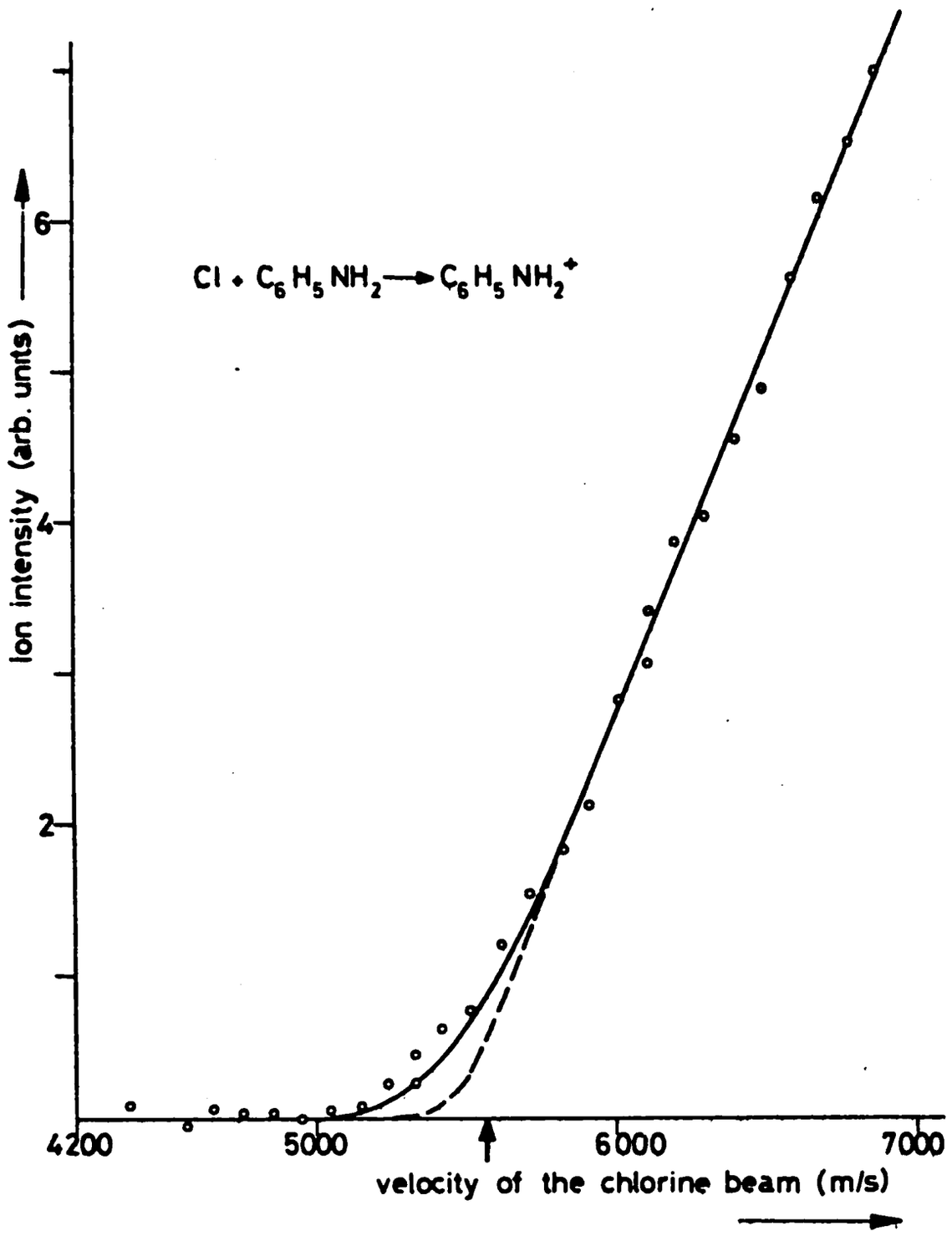

Fig. 6. Comparison of the model cross section for Cl on aniline with the experimental results. The dashed line represents the effect of the presence of different isotope combinations and excited states of the colliding particles on the ideal linear cross section. The solid line is the convolution of this curve with the resolution function of the velocity selector. The principal threshold (see text) is indicated by an arrow. The circles are the experimental points.

polated straight part of $\sigma_1(v)$ intersects the x-axis was calculated; this latter intersection is identical to the intersection of $\sigma_2(v_0)$, as mentioned above. By multiplication of the experimental intersection with this ratio, the value of the principle threshold velocity and therefore of the energy is known.

In fig. 6 the expected ionization yield $\sigma_2(v_0)$ is given for Cl and aniline as a solid line, together with a number of experimental points. $\sigma_2(v_0)$ is calculated by means of eq. (1) with a triangular resolution function $R(v)$ with $\Delta v/v = 10\%$. The dashed line in fig. 6 is the function $\sigma_1(v)$, so the expected cross section for a velocity selector with a δ shaped transmission. The principal threshold, indicated by an arrow, lies on the right hand of the experimental threshold.

The slight difference between the predicted curve and the experimental points is due to the velocity and angular spread of the thermal beam and the non-ideal alignment of the velocity selector, causing a somewhat worse resolution. These effects however do not change the intersection. For some of the experimental curves, there remains a small positive signal below threshold. This was treated as background and subtracted. Of course, this enlarges the experimental uncertainty.

In table 2 the experimental values of the principal threshold energies are given, together with the values known from photoionization [10]. In the second column of the halogen results the electron affinity EA of the halogen atoms [12] has been added to the principal threshold. The values thus obtained represent the minimum energy which must be put into a ground state aniline molecule in order to ionize, giving either the parent ion or breaking it up into the observed fragment plus a neutral rest. In our case, this energy is partly provided by the relative kinetic energy and partly by the electron affinity of the halogen atom. The values of the sum of the threshold and the electron affinity can be compared directly with the appearance potentials from mass spectroscopy.

4. Discussion

4.1. General

In table 3, the relative intensities of the various fragments of aniline formed in collisions with 17 eV Cl (our results) and 70 eV electrons [5] are compared.

These data are nearly equal, except for the mass 52 fragment. Due to the low resolution of the mass spectrometer in our experiment ($m/\Delta m \approx 20$), masses near the reported fragments might also give a contribution. At 17 eV it is likely that not all fragmentation thresholds will be reached. Therefore a simple mass spectrum of our aniline molecule can be expected. Consequently the mass peaks will have their main contribution from only one mass. The exception of mass 52 in table 3 may however be due to a contribution of one or two fragments differing in mass only one or two mass units.

It is surprising that the fragmentation spectrum for both processes in table 3 is so analogous. In case of electron impact it is believed that the only important variable for the fragmentation pattern is the amount of internal energy stored in the molecule. From table 3

Table 2
Threshold energies of charged fragments from ground state aniline ($C_6H_5NH_2$) formed by collisions with ground state halogen atoms and photons. In the second columns the electron affinity EA of the halogen atom is added to the threshold energy. EA is 3.45 eV for F, 3.61 eV for Cl, 3.36 eV for Br and 3.06 eV for I [12]

	F		Cl		Br		I		$h\nu$ [10]
Mass number	Threshold energy (eV)	Threshold + EA (eV)	Threshold energy (eV)	Threshold + EA (eV)	Threshold energy (eV)	Threshold + EA (eV)	Threshold energy (eV)	Threshold + EA (eV)	Threshold energy (eV)
93	4.18 ± 0.06	7.63 ± 0.06	7.69 ± 0.06	11.14 ± 0.06	4.36 ± 0.15	7.72 ± 0.15	4.4 ± 0.4	7.5 ± 0.4	7.67 ± 0.03
66	8.1 ± 0.3	11.5 ± 0.3	11.8 ± 0.2	15.2 ± 0.2	8.6 ± 0.3	12.0 ± 0.3	–	–	12.3 ± 0.1
52	–	–	13.1 ± 0.3	16.5 ± 0.3	–	–	–	–	–
39	–	–	13.1 ± 0.3	16.5 ± 0.3	–	–	–	–	–
28	–	–	17.0 ± 0.4	20.4 ± 0.4	–	–	–	–	–

Table 3
Relative intensities of charged fragments of aniline for 17 eV Cl impact and 70 eV electron impact

Ion mass	17 eV Cl	70 eV e^- [5]
93	100	100
66	32	33
52	16	5
39	17	18
28	9	8

we get the impression that the 17 eV Cl projectile deposits about the same amount of energy into the target aniline molecule as a 70 eV electron. The former particle dissipates a large amount of its kinetic energy into excitation of the aniline, the electron of 70 eV only a small part.

Comparison with photon impact is instructive. Fig. 7 shows the energy dependence of the photoionization cross section for the parent ion (mass 93) and the fragment ion with mass 66 for photon energies up to 14 eV, according to Akopyan and Vilesov [10]. The shape of the curves resembles our results (figs. 2–5). In Akopyan's photoionization curve we notice some structure, contrary to our results. Our lack of structure cannot be entirely due to the finite energy resolution (1 eV) of our velocity selector. This difference will be treated in section 4.3. From the similar fragmentation results for the different processes (electrons, photons or halogen impact) we conclude

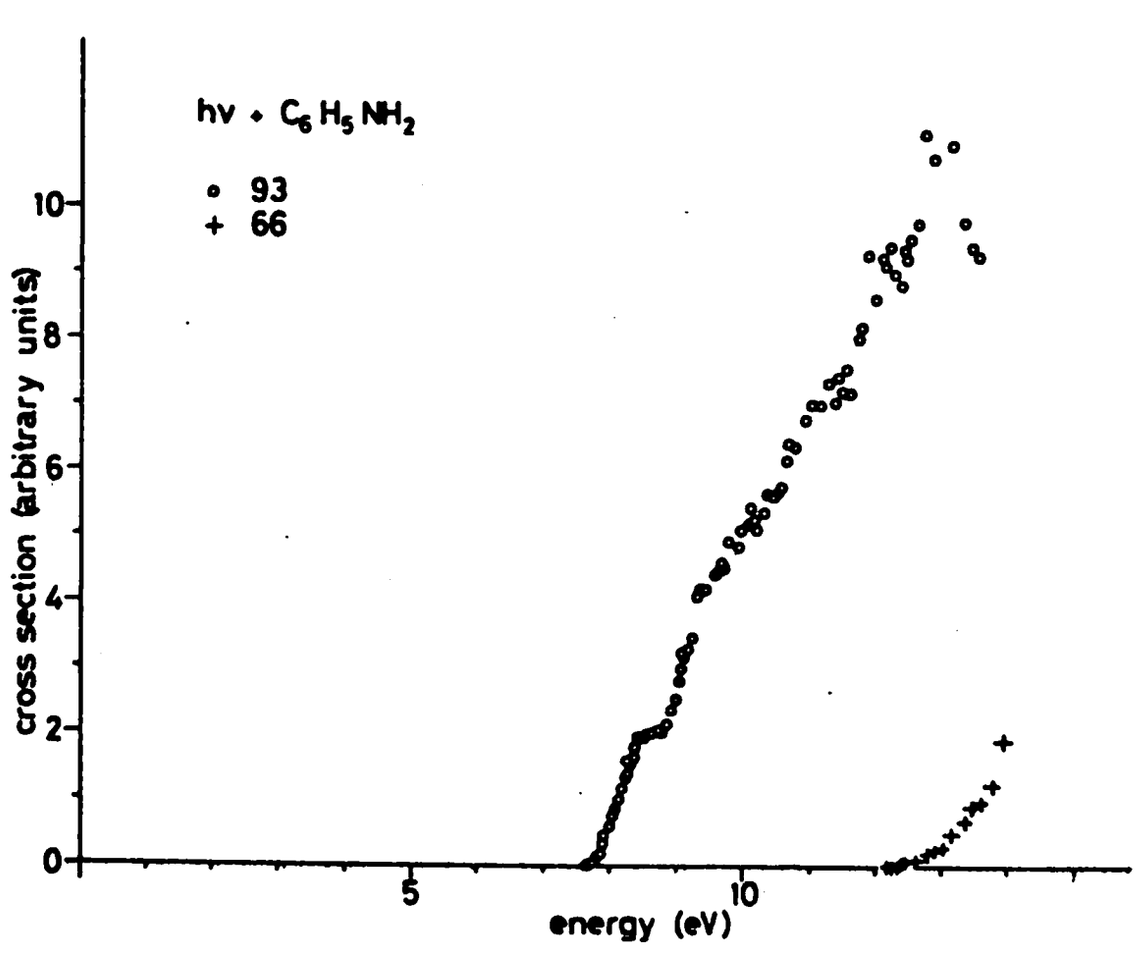

Fig. 7. Photoionization cross section for aniline, as reported by Akopyan and Vilesov [10].

that the formation of charged fragments in collisions with halogens proceeds in two steps. The first step is the formation of a positive molecular ion, which may contain excitation energy. Simultaneously a negative halogen ion is formed, as has been checked explicitly for Cl on aniline collisions up to 13 eV kinetic energy. The second step is a dissociative or radiative decay of the excited molecular ion, which also happens after the primary ionization by electron impact or photoionization. The possibility of dissociation of the molecular ion depends on its internal energy. In polyatomic ions vibrational and electronic energy quickly convert into each other via crossing points of the potential hypersurfaces of the ion. The ultimate fragmentation takes place from a vibrationally excited ion [16, 17]. This fragmentation is possible when the total available energy is larger than the dissociation energy of a particular bond. However, the energy is distributed over different bonds and has to be concentrated in the bond to be broken. Therefore, contrary to diatomic molecules, the time needed for dissociation (10^{-8} s) is very long compared to the collision time (10^{-13}–10^{-14} s). So the fragmentation pattern only depends on the total internal energy which is stored in the molecular ion [17]. This second step of the process has been discussed in many papers on the fragmentation of ions [16] and will not be treated further here. It occurs in exactly the same way with halogens as with electrons or photons. In the following we discuss the primary ionisation and excitation processes of aniline molecules in collisions with halogens, because these processes are different for the photon and electron impact phenomena.

4.2. Ionization and excitation processes

In photon and electron impact ionization the primary process is electron excitation according to the Franck–Condon principle. This excitation can cause direct emission of an electron (ionization), possibly accompanied by simultaneous excitation of a second electron. In heavy particle collisions, the ionization and excitation of the colliding particles is assumed to take place at a crossing of the potential curves or hypersurfaces of the quasi-molecule. Such an explanation may be applicable also for complicated molecules.

In fig. 8 a schematic diagram is shown of the relevant adiabatic potential energy curves for the Cl–aniline system. The energy given refers to the vibrational ground state of the molecule. Only the Coulomb interaction has been taken into account, intermolecular repulsions and the connected splittings are neglected; splittings due to spin have also been omitted. The x-axis represents the distance between the centers of charge of the particles rather than the intermolecular distance. The vertical dashed line is an estimate of the closest possible approach for relative kinetic energies of about 10 eV. Of course, the real potential energy also depends on the orientation of the aniline molecule.

The ionic curves cross the neutral curve in a certain point; the crossing point of ground state ions with ground state molecules is indicated by R_c. If the colliding particles pass R_c one time adiabatically and one time diabatically, they separate as a Cl^- ion and a positive aniline ion in its electronic ground state. This can only happen if the kinetic energy is larger than the difference between the neutral curve and the asymptote of the ionic curve.

In ion pair formation, this difference equals $I-EA$, I being the ionization potential of aniline molecules and EA the electron affinity of Cl atoms. For the formation of excited aniline ions, the system has to pass a second crossing point.

Repulsive forces will change the potential energy curves at short distances. This is schematically illustrated by the dashed curves in fig. 8 for the two lower energy states. Due to this effect, the potential energy of the crossing points will become higher, and may even be larger than $I - EA$. In the latter case, the threshold for ionpair formation is also larger than $I - EA$, since the system has to pass the crossing point to form ions. Then, just above threshold, the ionization cross section will be very small, since the classical turning point is near R_c. Consequently, the velocity at R_c is low and therefore the collision is almost completely adiabatic. Our curves however, start at $I-EA$ and have a steep rise immediately above threshold. Therefore in our systems the relevant crossing points lie below the asymptotes of the ionic curves.

In a complicated system like ours it is reasonable to assume that any of the crossing points can be passed both adiabatically and diabatically [17]. Of course, to get a transition, the kinetic energy has to be large enough to reach the crossing point. Therefore, crossings with very small internuclear separation will

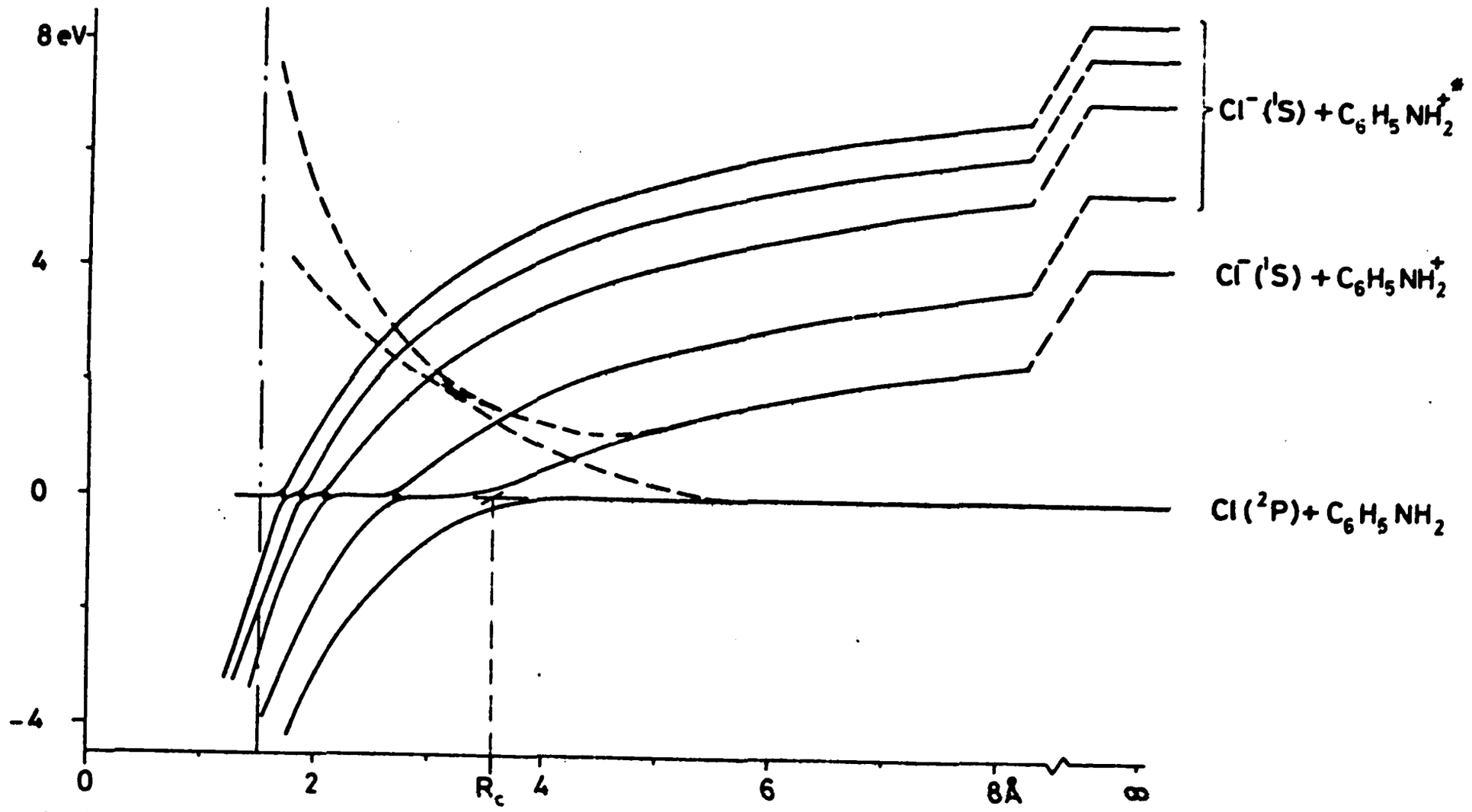

Fig. 8. Schematic diagram of the potential energy curves in the Cl–aniline system. For the ionic curves, the ground state potential curve as well as the first four excited states of the aniline ion [22] are given. Internuclear repulsion is neglected; the vertical dashed line represents an estimate of the closest possible approach. Splittings due to spin have not been drawn. R_c is the crossing point of the two lowest potential curves. For these curves, the influence of repulsive forces is roughly sketched by the dashed curves.

not contribute.

Little is known about the diabatic transition probability p at the crossing point. For simplicity, we consider the case that there are only two potential curves with one crossing point at R_c, where only radial coupling is relevant. Then, the transition probability is governed by the parameter $H_{12} = \langle 1|H|2\rangle$, in which $\langle 1|$ and $\langle 2|$ are the two diabatic electronic states and H is the electronic hamiltonian. Generally, the diabatic transition probability increases with velocity. If H_{12} is small, the diabatic transition probability will have a large value even at low energy. If on the other hand H_{12} is large, diabatic transitions are only frequent at high energy. Depending on the symmetry of the system, H_{12} may be zero. If this is not the case, H_{12} depends mainly on the crossing distance R_c.

For the Cl–aniline system we have, neglecting the non-coulombic forces: $I = 7.7$ eV, EA = 3.6 eV and $R_c = e^2/(I-\mathrm{EA}) = 3.5$ Å. Calculating H_{12} as in the case of two atoms, we find $H_{12} = 0.5$ eV [18]. The Landau–Zener formula can give an idea about the transition probability for such a system at a given velocity v. From this formula it follows that if

$$\gamma \equiv 2\pi H_{12}^2 / \left(\hbar v \frac{\mathrm{d}}{\mathrm{d}R}|H_{11}-H_{22}|_{R_c}\right) > 0.7$$

(H_{11} and H_{22} being the diabatic potential curves), the system behaves preferably adiabatically. At a crossing point of a coulombic potential curve with a covalent one,

$$\frac{\mathrm{d}}{\mathrm{d}R}|H_{11}-H_{22}|_{R_c} = e^2/R_c^2 ,$$

if the non-coulombic forces are neglected. Then, at a typical velocity of 10^4 m/s (13 eV Cl–aniline energy), γ is about 20. This means that the diabatic transition probability will be small for such a system at eV energies.

In atom–molecule collisions, the symmetry of the system depends on the relative orientation of the colliding particles. It may therefore happen that H_{12} is small for a given orientation, but has a large value for other configurations. If the impact occurs near the orientation with a low H_{12} value, the diabatic transition probability will be large even at low energies. Therefore, the total ionization cross section at low energy might be larger than in the atomic case. This will result in a smaller energy dependence of the cross section for formation of ions in a specific internal energy state than in atom–atom ion pair formation. Thus, one may expect that the cross section for formation of aniline ions in a given vibrational state might

be hardly energy dependent above its specific threshold. Then, the total cross section which represents the sum over all detailed cross sections is expected to be only considerably energy dependent near threshold, where new channels are opened with higher and higher internal energy of the aniline ion. Such a behaviour is indeed found experimentally in all aniline curves in figs. 2--5.

In the one-dimensional approximation, the cross section σ for ion pair formation is given by $\sigma = 2\pi R_c^2 p(1-p)$ (p being the diabatic transition probability). The halogen–aniline cross sections are only a few percent of those for $K-Br_2$ at 7000 m/s, where $p \approx 0.5$ [7]. For $K-Br_2$, $R_c = 8$ Å [7]. From this, the diabatic transition probabilities in our systems can be calculated to be at most 5%. Therefore, the cross sections for formation of excited aniline ions are expected to be very small, since for this at least two crossing points have to be passed diabatically.

4.3. The influence of internal energy levels

Information about the amount of the total excitation energy of the ions can be obtained from the experimental results. In a very simplified model, one neglects the energy dependence of the cross section for formation of ions in a given internal state. Then, in ion pair formation each channel with a given internal energy has an energy independent cross section above its specific threshold [19]. Within this model, the same holds for photoionization. The increase of the total ionization cross section is then only due to the population of new internal energy states of the ion. These states lie very closely together ($\ll 0.1$ eV [14]) and thresholds will therefore not be resolved. Then the first derivative of the gross ionization cross section (summed over all fragments) is proportional to the distribution of the internal energy over the various excited states of the ions [20]. The gross ionization cross section is given for Cl on aniline by the solid line in fig. 3. Since this cross section is nearly linear up to about 5 eV above threshold, it looks as if the distribution over the various internal energy levels is nearly uniform up to this energy. The further increase of the gross ionization cross section above 10 eV may be partly due to a trend of detailed cross sections to increase. From the fact that new fragments are formed with thresholds up to 10 eV above the parent ion threshold it can however be concluded that aniline ions with internal energy up to 10 eV are produced. Since the increase of the gross ionization cross section above 10 eV is mainly caused by the fragments, one gets the impression that even in this energy range the detailed cross sections are not very dependent on energy. Therefore, the first derivative of the gross ionization cross section seems to approximate the internal energy distributions of the aniline ions even at higher energies.

It is unlikely that the internal excitation is formed by electronic excitation alone. As mentioned before, this would require more than one diabatic transition through a crossing point. Since in our system the crossing points are dominantly passed adiabatically, such a process has a low probability. On the other hand, the collision times (about 5×10^{-14} s for 13 eV Cl) are in the same order of magnitude as the vibration times in the molecule (about 3×10^{-14} s [14]), and vibrational excitation is thus a likely process. Part of the internal energy therefore is probably formed as vibration. Since multiquantum transitions take place at these energies even for di- and triatomic molecules [21], the total vibrational excitation of a complicated molecule like aniline may perhaps reach some eV's.

In photoionization, the vibrational levels are populated according to the Franck–Condon principle. The distribution function of the internal energy then shows a very marked structure [22]. Collisional excitation will be less selective and consequently the distribution function might be rather flat. Since the cross section equals roughly the integral of the internal energy distribution function, also no marked structure is to be expected in the ionization cross section. This corresponds with the absence of any structure in our measurements contrary to those at 8.4 eV in the photoionization curve.

As can be seen from table 2, the sum of the threshold energy for the mass 66 fragment and the electron affinity of the halogens is about 0.5 eV lower than the photoionization threshold. This latter value however equals the 66^+ thresholds in electronbombardment [23]. This discrepancy might be understood as follows. Since the photoionization spectrum of aniline shows a maximum at 11.8 eV [22], it follows that in photoionization aniline ions with internal energy corresponding to the halogen process are indeed produced.

If however the free conversion of the excited state corresponding to this maximum with lower levels is hindered, the mass 66 fragment will not be formed in photoionization, even though the energy content of the aniline ion is sufficient for formation of this fragment. In halogen collisions however, other states than in photoionization or electron bombardment ionization may be populated during collision, which do lead to production of the mass 66 fragment at our experimental thresholds.

Acknowledgement

We thank Dr. N.M.M. Nibbering for the determination of the chemical formula of the mass 66 fragment ion of aniline.

This work is part of the research program of the Stichting voor Fundamenteel Onderzoek der Materie (Foundation of Fundamental Research on Matter) and was made possible by financial support of the Nederlandse Organisatie voor Zuiver-Wetenschappelijk Onderzoek (Netherlands Organization for the Advancement of Pure Research).

References

[1] A.P.M. Baede, Advan. Chem. Phys., to be published;
J. Los, in: The physics of electronic and atomic collisions, VIII ICPEAC, eds. B. Cobić and M.V. Kurepa, Beograd, 1973 (Institute of Physics, Beograd);
S. Wexler, Ber. Bunsenges. Phys. Chem. 77 (1973) 606.

[2] G.P. Können, J. Grosser, A. Haring, A.E. de Vries and J. Kistemaker, Rad. Eff. 21 (1974) 171.

[3] J. Politiek, P.K. Rol, J. Los and P.G. Ikelaar, Rev. Sci. Instr. 39 (1968) 1147.

[4] A.P.M. Baede, D.J. Auerbach and J. Los, Physica 64 (1973) 134.

[5] Americal Petroleum Institute, Research number 44 "Catalog of mass spectra data".

[6] M.M. Hubers, private communication.

[7] A.P.M. Baede and J. Los, Physica 52 (1971) 422.

[8] P.N. Rylander, S. Meyerson, E.L. Eliël and J.D. McCollum, J. Am. Chem. Soc. 85 (1963) 2723.

[9] Mass Spectroscopy Data Centre AWRE, Aldermaston, Berks.

[10] M.E. Akopyan and V.I. Vilesov, Dokl. Akad. Nauk SSSR, 158 (1964) 1386.

[11] N.M.M. Nibbering, private communication.

[12] Handbook of Chemistry and Physics, 1972–1973.

[13] C.E. Moore, Atomic Energy Levels, NBS Circul. 467, Vol. 1 (1949), Vol. 2 (1952), Vol. 3 (1958) (US Govnt. Printing Office, Washington).

[14] G. Herzberg, Infrared and Raman spectra (Van Nostrand, New York, 1959).

[15] A.P.M. Moutinho, Thesis, University of Leiden (1971).

[16] See, for example, M.L. Vestal, in: Fundamental processes in radiation chemistry, ed. P. Ausloos (Wiley–Interscience, New York, 1970).

[17] B. Steiner, C.F. Giese and M.G. Ingram, J. Chem. Phys. 34 (1961) 189.

[18] R.E. Olson, F.T. Smith and E. Bauer, Appl. Opt. 10 (1971) 1848.

[19] E.P. Wigner, Phys. Rev. 73 (1948) 1002.

[20] J.D. Morrison, J. Appl. Phys. 28 (1957) 1409.

[21] J.N. Bass, J. Chem. Phys. 60 (1974) 2913;
H. Udseth and C.F. Giese, J. Chem. Phys. 54 (1971) 3642.

[22] D.W. Turner, Molecular photoelectron spectroscopy (Wiley–Interscience, New York, 1970).

[23] R. Frey and B. Brehm, private communication.